

Effects of Evaporation and Thermocapillary Convection on Volatile Liquid Droplets

David F. Chao*

NASA John H. Glenn Research Center at Lewis Field, Cleveland, Ohio 44135

and

Nengli Zhang†

Ohio Aerospace Institute, Cleveland, Ohio 44142

Results of an experimental investigation of evaporating sessile drops on a glass-slide surface for three volatile liquids show that both evaporation and thermocapillary convection in the sessile drop strongly affect the drop spreading and contact angle. The evolution of contact diameter of the drops can be divided into four stages: 1) initial spreading, 2) spreading–evaporation balance, 3) evaporation–dominating contraction, and 4) final rapid contraction. Molecular-kinetic spreading always occurs in the early first stage and is rapidly restrained and then taken over by the effects of evaporation. Thermocapillary convection, induced by the evaporation, promotes the competition of evaporation over the spreading and shortens the spreading–evaporation balance stage to become undetectable. Evaporation may increase or decrease the contact angle of the evaporating sessile drops, depending on the evaporation rate.

Introduction

THE spreading of a liquid on a solid surface plays an important role in many industrial and material processing operations, such as painting, coating, soldering, gluing, lubricating, mold filling, film cooling, and boiling heat transfer. It is also a concern in performance of fuel tanks in space applications.

Spreading of nonvolatile liquid droplets has been well studied by many investigators, and a comprehensive review was made by Leger and Joanny.¹ The lack of volatility of the liquid implies the conservation of mass and volume and, thus, simplifies the theoretical analysis. The occurrence of evaporation of common liquids, however, is inevitable as long as the environment in the close vicinity of a droplet is not saturated with the vapor of the liquid. An understanding of the evaporation effects on the contact angle of a droplet is important in the study of the spreading of volatile liquids. Unfortunately, both experimental and theoretical studies on this subject are still lacking.

Picknett and Bexon² studied evaporation modes both theoretically and experimentally. They distinguished two extreme modes of evaporation: constant-angle mode and constant-contact-area mode. They observed both of these two basic modes and a mixed mode in their experiments. Birdi et al.³ investigated the evaporation rate of a sessile drop of water resting on a smooth solid surface. They found that the rate of evaporation is constant and depends on the radius of the liquid–solid interface. It is also found that the radius of the liquid–solid interface remains constant, while the contact angle decreases during evaporation. Shanahan and Bourges⁴ and Bourges–Monnier and Shanahan⁵ conducted experiments of sessile drops of water and *n*-decane placed on various substrates. In these experiments, the beginning atmosphere was the saturated vapor, followed by an atmosphere of reducing vapor content. They divided the process into four stages and concluded that the evaporation of the liquid from the drop meniscus lowers the contact angle. Rowan et al.⁶ studied the rate of evaporation of small water droplets on a poly-methyl methacrylate surface and concluded that in the regime

of constant contact radius the height and the contact angle reduce linearly with time approximately.

Most investigators focus attention on the effect of evaporation on the contact angle during the major portion of the drop evolution process, ignoring the spreading in the initial stage. Anderson and Davis⁷ analytically studied the spreading of volatile liquid droplets on heated surfaces and found that for the case of zero capillary number (non-viscous liquids), there are two basic regimes in which the dynamics of the contact line differ: 1) a strong-evaporation regime characterized by a monotonic decreasing of droplet radius in time and 2) a weak-evaporation regime characterized by the initial droplet spreading. For small but nonzero capillary number, they found that thermocapillary action tends to contract the droplet through transport of mass from the contact-line region toward the droplet center. As they noted, the Marangoni flow observed in their case is directly opposite that observed by Cazabat et al.⁸ and Redon et al.⁹ In fact, Marangoni flow has a complex structure that was experimentally revealed by Zhang and Yang.^{10–12} Generally, in the main portion of the sessile drop, the liquid flows from the summit toward the periphery of the drop along the surface and returns to the center along the base of the drop, forming thermocapillary convection. Meanwhile, a ring of roll cells runs in the contact-line region.

Recently, Hocking¹³ considered that the macroscopic contact angle deviates from the microscopic angle in the slip region and found that the contact angle is increased by evaporation. However, Shanahan and Bourges⁴ and Bourges–Monnier and Shanahan⁵ concluded that evaporation from the drop meniscus lowers the contact angle, whereas Moosman and Homsy¹⁴ and Sujjanani and Wayner¹⁵ reported an increase in the contact angle when evaporation is present. All available studies considered that the capillary spreading of the drop is in competition with the loss of liquid volume in the drop through evaporation. Unfortunately, it is not at all clear which mechanism is dominant. The puzzle may arise from ignoring the effects of Marangoni convection induced by evaporation on the spreading and the contact angle of sessile drops.

In this paper, we report the results of an experimental study on spreading of volatile liquid drops, with different evaporation rates, on a glass slide, and show the effects of evaporation and thermocapillary convection in sessile drops on the spreading rate and the contact angle of the drops.

Experimental Method

A hybrid optical system of laser shadowgraphy and direct photography, developed by Zhang and Chao,^{16,17} is used in the present

Received 16 October 2000; revision received 28 February 2001; accepted for publication 4 April 2001. Copyright © 2001 by the American Institute of Aeronautics and Astronautics, Inc. No copyright is asserted in the United States under Title 17, U.S. Code. The U.S. Government has a royalty-free license to exercise all rights under the copyright claimed herein for Governmental purposes. All other rights are reserved by the copyright owner.

*Research Scientist, Microgravity Science Division, Mail Stop 500-102.

†Senior Scientist, Department of Workforce Enhancement.

study. The hybrid optical system is shown schematically in Fig. 1. A laser beam and a white-light beam are collimated to horizontally parallel beams and then reflected by a splitter to pass perpendicularly through a test drop, situated on a microscope slide, without obstructing the top view of the drop. The laser beam produces a refractive image of the sessile drop on a screen, and the white beam provides a sharp photograph of the top view of the drop. The refractive image on the screen is recorded by a video system (system 1) that consists of a charge-coupled device (CCD) zoom camera, a video recorder, and a monitor. A second video system (system 2) records the top view of the sessile drop. Both recording systems can replay frame-by-frame at 30 frames/s.

Before each test, the glass slide is cleaned by ethanol and wiped by lens-cleaning tissue, and then shelved in open air, covered by a soft tissue, for at least 24 h. The slide surface becomes free of residual liquid molecules while remaining free of impurities from the ambient air. The test liquid is carefully deposited on the slide by a microsyringe to form a 1.5–2.5 μl sessile drop. The origin of spreading and evaporation time is taken as the moment when the microsyringe is detached from the liquid body. Typical photographs of the top view and the refractive image of an n-pentane sessile drop are shown in Fig. 2, which were taken at 0.5 s from the beginning of the spreading for the drop with an initial volume 1.61 μl .

The evolution of the contact diameter of the drop, $d(t)$, is directly measured from the magnified top views as recorded by video system 2 to an accuracy of ± 0.02 mm. Because the test drops are quite small and almost nondeforming by gravitational force, the drops can be considered to be sphere caps without significant error.⁴ The method developed by Zhang and Yang¹⁸ is used to determine the instantane-

ous contact angle $\theta(t)$. By a very simple geometric relationship, the following expression can be derived:

$$\theta(t) = \arcsin[d(t)/2R(t)] \quad (1)$$

where $R(t)$ is the curvature radius of the liquid sphere cap at moment t , which, assuming the sessile drop is a lens, can be calculated by

$$R(t) = (n - 1)s \frac{d(t)}{D(t) + d(t)} \quad (2)$$

where n is the refractive index of the test liquid, s is the distance measured from the contact base center of the tested drop via the mirror to the screen, that is, AB + BC shown in Fig. 1, and $D(t)$ is the instant diameter of the outmost fringe ring of the drop refractive image on the screen. The average evaporation rate of a sessile drop, \bar{w} , is taken as a parameter measuring the evaporation strength and can be determined by

$$\bar{w} = V_0/t_f \quad (3)$$

where V_0 is the initial volume of the sessile drop (the drop volume at $t = 0$) and t_f is the lifetime of the tested drop. Note that, because of liquid evaporation and wetting on the needle of the syringe, the scale on the microsyringe could not be used to measure accurately the initial volume of the tested drop. The laser shadowgraphy method can determine the drop volume at any moment by the following equation:

$$V(t) = \pi h^2(t) \{R(t) - [h(t)/3]\} \quad (4)$$

where $h(t)$ is the maximum height of the sessile drop at moment t , determined by

$$h(t) = R(t) - \sqrt{R^2(t) - [d^2(t)/4]} \quad (5)$$

It can be seen that only two basic parameters, that is, $d(t)$ and $D(t)$, are needed to be measured.

Experimental Results

Three volatile liquids, cyclohexane, n-pentane, and freon-113 (R-113), are tested in open air at room temperature (23°C) and relative humidity of 44%. The initial volume of the sessile drops is controlled to less than 2.5 μl and, therefore, the drop profiles can be taken as sphere caps. Experimental results show that both the evaporation rate and Marangoni convection induced by the evaporation strongly affect the spreading. Although the average evaporation rates between the tested liquids differ by an order of magnitude, in all cases, the capillary spreading dominates the initial stage and

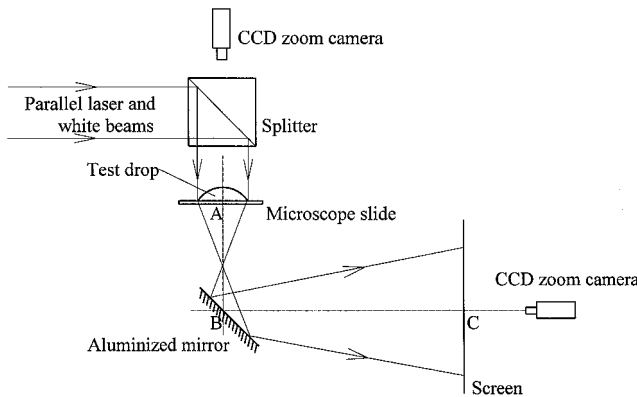


Fig. 1 Hybrid optical system for measurements of drop spreading and contact angle.

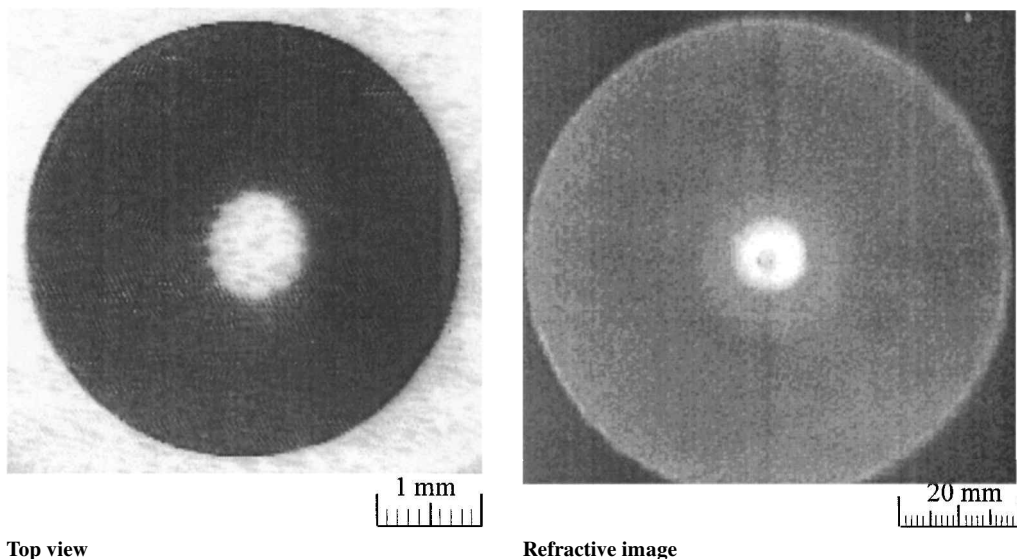


Fig. 2 Typical pictures of the top view and the corresponding refractive image of an n-pentane sessile drop.

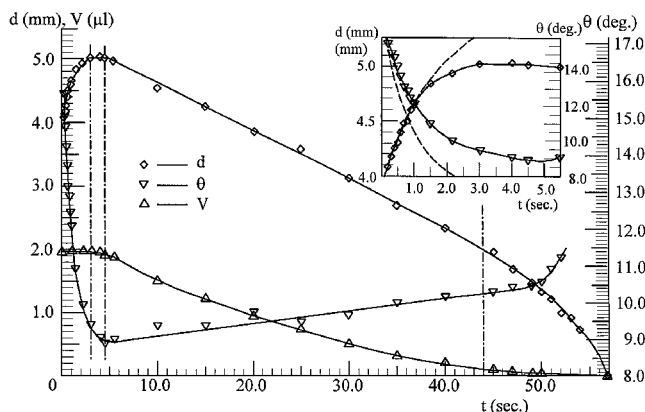


Fig. 3 Evolution of drop contact diameter, contact angle, and volume for a cyclohexane drop of initial volume $1.91 \mu\text{l}$.

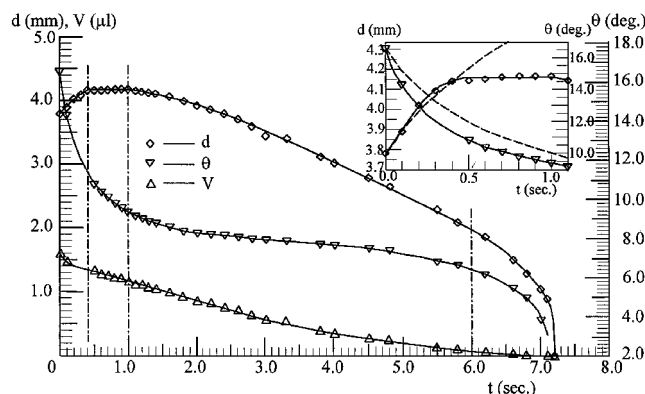


Fig. 4 Evolution of drop contact diameter, contact angle, and volume for an n-pentane drop of initial volume $1.61 \mu\text{l}$.

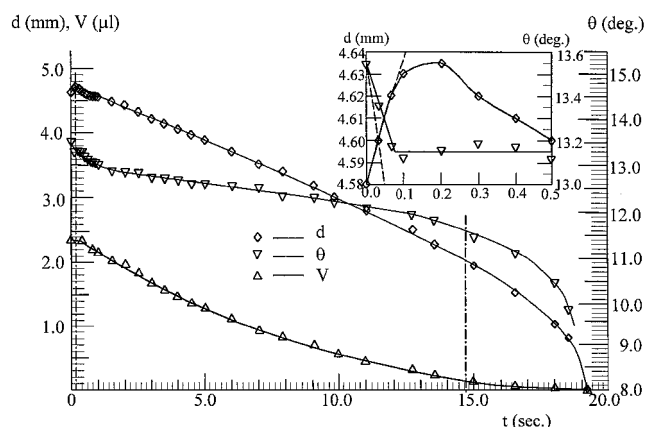


Fig. 5 Evolution of drop contact diameter, contact angle, and volume for an R-113 drop of initial volume $2.36 \mu\text{l}$.

is gradually overtaken by the effect of evaporation, as shown in Figs. 3–5.

Effects of Evaporation Rate

The results clearly indicate that the evaporation rate strongly affects the spreading of sessile drops. Generally, after a short initial spreading period, the drop approximately maintains a constant contact diameter for a brief period that is followed by a monotonic contraction. Four stages are observed: 1) initial spreading, 2) spreading–evaporation balance, 3) evaporation-dominant contraction, and 4) rapid contraction. The higher the evaporation rate is, the shorter the initial spreading. Typical cases are described as follows. A cyclohexane sessile drop of initial volume $1.91 \mu\text{l}$ has a lifetime

56.83 s, with an average evaporation rate of $0.034 \mu\text{l/s}$. Initially, the drop rapidly spreads, its contact diameter expands from 3.81 to 5.01 mm within 3 s, then the contact diameter remains unchanged for about 1.5 s as the effects of evaporation and spreading reach a balance. Evaporation then dominates the process where the drop almost linearly contracts to about 2 mm in contact diameter and then rapidly contracts until vanishing, as shown in Fig. 3. Correspondingly, an n-pentane sessile drop has a much higher evaporation rate and a shorter spreading period. For example, an n-pentane drop with an initial volume of $1.61 \mu\text{l}$ has a lifetime of 7.2 s, with an average evaporation rate of $0.22 \mu\text{l/s}$. The drop has the same evolution behavior of the contact diameter as the cyclohexane drop, but spreads for only 0.4 s, as shown in Fig. 4. Note that the final rapid contraction stage starts at the same contact diameter of about 2 mm.

To demonstrate the characteristics of the spreading behavior of the evaporating sessile drops, a comparison is made with nonvolatile liquid drops. It is well known that there exist two different types of sessile droplet spreading behavior: hydrodynamic and molecular kinetic. The first is characterized by $d(t) \sim t^{1/10}$ and $\theta(t) \sim t^{-3/10}$ and the second by $d(t) \sim t^{1/7}$ and $\theta(t) \sim t^{-3/7}$. Recently, using a combined dissipation channel approach, de Ruijter et al.¹⁹ found that a succession of four different regimes exist in general cases, namely, 1) a fast early-time stage of a linear time dependence of the contact diameter, 2) a molecular-kinetic stage, 3) a hydrodynamic stage, and 4) an exponential relaxation stage. Note that the fast early-time stage is quite short, as estimated by de Ruijter et al., to be only 0.008 s from the experimental data they cite. Therefore, the fast early-time stage can be reasonably ignored, and the molecular-kinetic stage can be taken as the first stage. Dodge's²⁰ test results show that the spreading follows $d = k(t + a)^{1/7}$, where k and a are experimental constants. Following Dodge's relation, the spreading behavior of a nonvolatile liquid sessile drop, with the same initial volume, is plotted by dashed lines in the insets in the upper right corners of Figs. 3–5. It can be seen that in the first half-period of the initial spreading stage, the drop spreading follows Dodge's relation and then rapidly deviates from molecular-kinetic spreading under the effects of evaporation with a tendency to contract.

Note that, although the evaporation rate of R-113 sessile drops is lower than that of n-pentane sessile drops, the initial spreading stage of an R-113 drop is much shorter than that of an n-pentane drop. This implies that there is another physical process that affects the evolution of the contact diameter.

Effects of Thermocapillary Convection

Previous experiments reveal that evaporation could induce convection inside sessile drops.^{10–12} Recently, Chai and Zhang²¹ and Zhang and Chao²² experimentally demonstrated that, in an evaporating thin layer, evaporation not only produces a temperature gradient but also is a direct driving force inducing and sustaining the thermocapillary convection. The effect of convection on the spreading of sessile drops has not been investigated. In the present study, it is shown that the thermocapillary convection induced by evaporation has pronounced effects on the spreading of sessile drops.

Thermocapillary convection in sessile drops can be induced by evaporation only under certain conditions, depending on the properties of the volatile liquids. Of the three liquids tested in this study, the cyclohexane drops, with initial volumes of $1.5\text{--}5 \mu\text{l}$, exhibit no convection throughout their lifetimes. The convection in n-pentane drops occurs near the end of the second stage (the spreading–evaporation balance stage). For example, for the n-pentane drop with an initial volume of $1.61 \mu\text{l}$, convection appears at about 1 s after the drop begins to spread, as shown in Fig. 6a. Before then there is no convection in the drop at all, as shown in Fig. 2a, which was taken at 0.5 s from beginning of the drop spreading. On the other hand, the thermocapillary convection in the R-113 sessile drops is induced by evaporation from the very beginning, even before the syringe detaches from the drops. The convection in the R-113 drops is considerably stronger than in the n-pentane drops, as shown in Fig. 6b, which was taken at 0.2 s.

Because of the strong thermocapillary convection in the R-113 sessile drops, the evolution of the contact diameter is different from

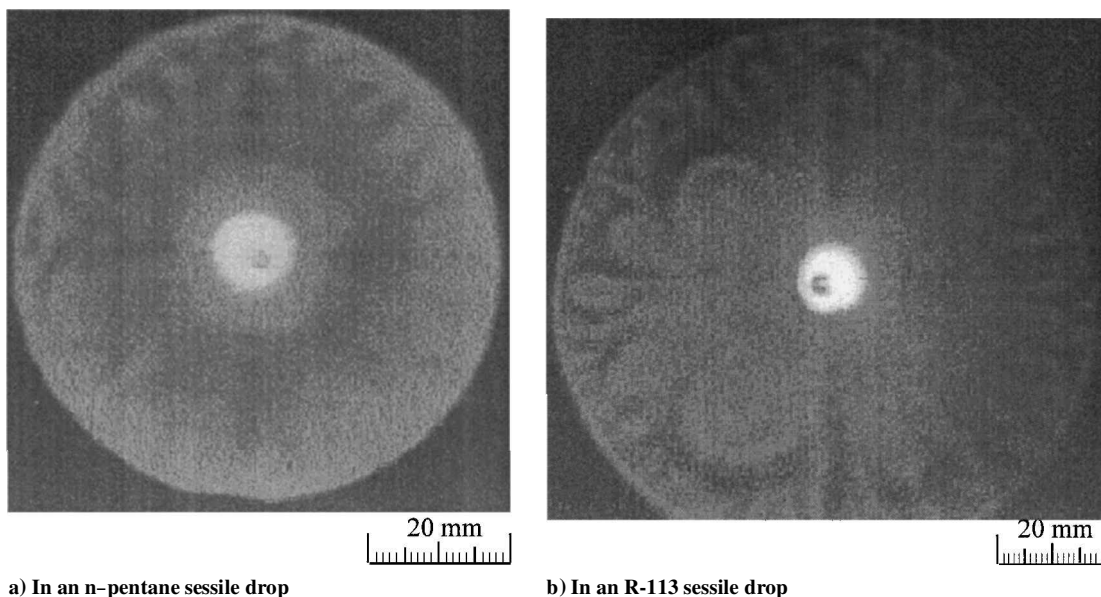


Fig. 6 Refractive images of thermocapillary convection in a sessile drop at the beginning of the evaporation dominating contraction stage.

that of both cyclohexane and n-pentane drops. From Fig. 5, it is evident that, for the R-113 sessile drop with an initial volume of $2.36 \mu\text{l}$, the initial spreading stage is quite short (0.2 s), though the evaporation rate of the R-113 drop ($0.12 \mu\text{l/s}$) is much lower than n-pentane. Also note that no spreading–evaporation balance stage is observed. This means the thermocapillary convection in sessile drops prevents the drops from spreading, promoting evaporation over the molecular-kinetic spreading in the evolution of contact diameter. Note that the R-113 drop accelerates contraction after its contact diameter reaches 2 mm.

Evolution of Contact Angle

The evolution of contact angle of a sessile drop is quite different among the various liquids.

For drops with lower evaporation rates, the contact angle decreases in the initial spreading and the spreading–evaporation balance stages. It increases linearly in the evaporation-dominant contraction stage and then rapidly grows in the final rapid-contraction stage, as shown in Fig. 3. Note that, in the initial spreading stage, the evaporation rate is small, and the spreading follows Dodge's relation²⁰ in the early initial spreading stage. Contrarily, the contact-angle evolution pronouncedly deviates from the relation between contact angle and spreading velocity, which suggests $\theta \sim d^{-3}$ for nonvolatile liquid sessile drops.^{19,20} The evolution of contact angle in the initial spreading stage determined by the relation of $\theta \sim d^{-3}$ for nonvolatile liquid sessile drops is plotted by dashed line in the detail of Fig. 3. Obviously, evaporation increases the contact angle because of a large evaporative loss near the drop edge, which is qualitatively in agreement with the theoretical predictions of Anderson and Davis⁷ and Hocking.¹³

For the drops with higher evaporation rates, the contact angle decreases monotonically and has a contact-angle plateau in the evaporation-dominant contraction stage (see Figs. 4 and 5). Although the evaporation generally would increase the contact angle, at the point where the stronger evaporation consumes the liquid volume of the drop large enough the contact angle starts to decrease. The characteristics of the evolution of the contact diameter and the contact angle shown in Figs. 4 and 5 surprisingly resemble the theoretical prediction for the weak evaporation regime proposed by Anderson and Davis (see Figs. 6 and 7 in Ref. 7). Note that the weak evaporation defined by Anderson and Davis does not mean a lower evaporation rate. For example, ethanol unequivocally has a higher evaporation rate than water, but the former is weaker than the latter according to the definition and the data in Table I in Ref. 7.

The effects of evaporation rate on the contact angle in the initial spreading stage can be seen clearly in the insets in the upper right corners of Figs. 3–5. Comparing to the evolution curves of contact angle plotted from relation $\theta \sim d^{-3}$ for nonvolatile liquid drops (dashed lines), the contact angle for the drop with the lower evaporation rate is obviously larger, whereas for the drop with the higher evaporation rate, it is smaller. Strong thermocapillary convection may also cause the contact angle to increase.

Uncertainty Analysis

The method of single sample experiments was utilized to estimate the uncertainties in both θ and V through Eqs. (1) and (4). The maximum uncertainty occurs in the end of the final stage for R-113 sessile drop, in which $d = 0.82 \pm 0.019 \text{ mm}$ and $D = 76.2 \pm 0.22 \text{ mm}$. The uncertainty for the contact angle is 2.78% and for the drop volume is 10.68%, respectively.

Conclusions

Experimental results of evaporating sessile drops on a glass-slide surface for three volatile liquids show that both evaporation and thermocapillary convection strongly affect the drop spreading and contact angle. The main conclusions are summarized as follows:

- 1) An evolution of contact diameter of a sessile drop can be divided into four stages: a) initial spreading, b) spreading–evaporation balance, c) evaporation-dominant contraction, and d) rapid contraction.
- 2) Molecular-kinetic spreading always exists at the early initial spreading stage in the evolution of contact diameter of an evaporating liquid sessile drop, even if the drop has a considerably high-evaporation rate, but is rapidly taken over by the effects of evaporation. The evolution of the contact diameter of an evaporating sessile drop in the early initial spreading stage follows Dodge's relation.²⁰
- 3) Thermocapillary convection promotes the evaporation over the spreading and shortens the spreading–evaporation balance stage to become undetectable.
- 4) The contact angle of sessile drops with low-evaporation rate is increased by evaporation. However, strong evaporation decreases the contact angle to create a contact-angle plateau in the evaporation-dominant contraction stage as predicted by Anderson and Davis.⁷
- 5) The evaporation of sessile drops always accelerates contraction after their contact diameter reaches 2 mm.

References

- ¹ Leger, L., and Joanny, J. F., "Liquid Spreading," *Reports on Progress in Physics*, Vol. 55, No. 4, 1992, pp. 431–486.

- ²Picknett, R. G., and Bexon, R. J., "The Evaporation of Sessile or Pendant Drops in Still Air," *Journal of Colloid and Interface Science*, Vol. 61, No. 2, 1977, pp. 336–350.
- ³Birdi, K. S., Vu, D. T., and Winter, A., "A Study of the Evaporation Rates of Small Water Drops Placed on a Solid Surface," *Journal of Physical Chemistry*, Vol. 93, No. 9, 1989, pp. 3702, 3703.
- ⁴Shanahan, M. E. R., and Bourges, C., "Effects of Evaporation on Contact Angles on Polymer Surfaces," *International Journal of Adhesion and Adhesives*, Vol. 14, No. 3, 1994, pp. 201–205.
- ⁵Bourges-Monnier, C., and Shanahan, M. E. R., "Influence of Evaporation on Contact Angle," *Langmuir*, Vol. 11, No. 7, 1995, pp. 2820–2829.
- ⁶Rowan, S. M., Newton, M. I., and McHale, G., "Evaporation of Microdroplets and the Wetting of Solid Surfaces," *Journal of Physical Chemistry*, Vol. 99, No. 35, 1995, pp. 13268–13271.
- ⁷Anderson, D. M., and Davis, S. H., "The Spreading of Volatile Liquid Droplets on Heated Surfaces," *Physics of Fluids*, Vol. 7, No. 2, 1995, pp. 248–265.
- ⁸Cazabat, A. M., Heslot, F., Troian, S. M., and Carles, P., "Fingering Instability of Thin Spreading Films Driven by Temperature Gradients," *Nature*, Vol. 346, No. 6287, 1990, pp. 824–826.
- ⁹Redon, C., Brochard-Wyart, F., and Rondelez, F., "Festoon Instabilities of Slightly Volatile Liquids During Spreading," *Journal of Physics II France*, Vol. 2, Sept. 1992, pp. 1671–1676.
- ¹⁰Zhang, N., and Yang, W. J., "Evaporation and Explosion of Liquid Drops on a Heated Surface," *Experiments in Fluids*, Vol. 1, No. 2, 1983, pp. 101–111.
- ¹¹Zhang, N., and Yang, W. J., "Evaporative Convection in Minute Drops on a Plate with Temperature Gradient," *International Journal of Heat and Mass Transfer*, Vol. 26, No. 10, 1983, pp. 1479–1487.
- ¹²Zhang, N., and Yang, W. J., "Microstructure of Flow Inside Minute Drops Evaporating on a Surface," *Journal of Heat Transfer*, Vol. 105, No. 4, 1983, pp. 908–910.
- ¹³Hocking, L. M., "On Contact Angles in Evaporating Liquids," *Physics of Fluids*, Vol. 7, No. 12, 1995, pp. 2950–2955.
- ¹⁴Moosman, S., and Homsy, G. M., "Evaporating Menisci of Wetting Fluids," *Journal of Colloid and Interface Science*, Vol. 73, No. 1, 1980, pp. 212–223.
- ¹⁵Sujanani, M., and Wayner, P. C., Jr., "Transport Processes and Interfacial Phenomena in an Evaporating Meniscus," *Chemical Engineering Communication*, Vol. 118, No. 1, 1992, pp. 89–110.
- ¹⁶Zhang, N., and Chao, D. F., "A New Approach to Measure Contact Angle and Evaporation Rate with Flow Visualization in a Sessile Drop," International Conf. on Interface Problem, Aug. 1999; also NASA/TM-1999-209636, 1999.
- ¹⁷Zhang, N., and Chao, D. F., "Effects of Evaporation/Condensation on Spreading and Contact Angle of a Volatile Liquid Drop," *Proceedings of the 5th International Symposium on Heat Transfer*, Aug. 2000, pp. 367–372.
- ¹⁸Zhang, N., and Yang, W. J., "Natural Convection in Evaporating Minute Drops," *Journal of Heat Transfer*, Vol. 104, No. 2, 1983, pp. 656–662.
- ¹⁹de Ruijter, M. J., De Coninck, J., and Oshanin, G., "Droplet Spreading: Partial Wetting Regime Revisited," *Langmuir*, Vol. 15, No. 6, 1999, pp. 2209–2216.
- ²⁰Dodge, F. T., "The Spreading of Liquid Droplets on Solid Surfaces," *Journal of Colloid and Interface Science*, Vol. 121, No. 1, 1988, pp. 154–160.
- ²¹Chai, A. T., and Zhang, N., "Experimental Study of Marangoni-Benard Convection in a Liquid Layer Induced by Evaporation," *Experimental Heat Transfer*, Vol. 11, No. 3, 1998, pp. 187–205.
- ²²Zhang, N., and Chao, D. F., "Mechanisms of Convection Instability in Thin Liquid Layers Induced by Evaporation," *International Communications in Heat and Mass Transfer*, Vol. 26, No. 8, 1999, pp. 1069–1080.